it is possible, assuming such a distribution, to derive expressions which fit the observed values for the complex bulk modulus at various temperatures. The compressional and shear viscosities are also found to be equal within experimental error, suggesting that a structural mechanism is responsible for the observed properties. This does not necessarily contradict the assumptions of the present paper, since we have assumed here that the theoretical model to be used at temperatures substantially below room temperature, where large molecular aggregates may occur, as suggested by Yoshida,[4] is quite different from that applying at room temperature and above. It is only in the latter region that a thermal mechanism should be considered, since the vibrational relaxation time will be very long at lower temperatures.

PHYSICAL REVIEW VOLUME 106, NUMBER 4 MAY 15, 1957

Spectrum of Target Bremsstrahlung at Small Angles*†

A. SIRLIN
Laboratory of Nuclear Studies, Cornell University, Ithaca, New York
(Received February 7, 1957)

The combination of Schiff's energy-angle distribution for the radiated photons and a Gaussian-like theory of multiple scattering for the incident electrons is studied. The emphasis here is placed on a detailed consideration of the influence of screening as expressed in the Schiff's theory.

An expression for the forward radiation is first developed, which is valid for values of $\lambda \ll 1$ and for any value of ρ (λ and ρ being parameters which essentially measure the importance of multiple scattering and screening, respectively). This result shows that the deviations of the actual forward spectrum from the integrated spectrum of the intrinsic distribution are appreciable even for small values of λ, the corrections being largest for complete screening and negligible for no screening.

The case of complete screening is then studied exactly both for the forward radiation and the angular distribution. The latter results show that the integrated spectrum approximation is a good one when $\theta \gtrsim \mu/E_0$ and $\lambda \ll 1$. In a particular case, the theory predicts that the angular distribution (normalized to unity at $\theta=0$) is somewhat broader for complete screening than for no screening.

An exact treatment of the forward radiation is given for the cases of complete screening and no screening. Finally, an expression is developed, which yields the same result as the exact treatment for complete screening and no screening and provides a good approximation for intermediate screening.

INTRODUCTION

In a recent paper, the angular distribution of bremsstrahlung from targets of moderate thickness (which are frequently used in betatrons and synchrotrons) was studied on the basis of Schiff's energy-angle distribution for the radiated photons and Molière's complete theory of multiple scattering for the incident electrons.[1–3]

The necessity of using an expression based on the complete theory of multiple scattering in order to obtain accurate agreement with experiment at moderate and relatively large angles ($\vartheta \gtrsim 1$) was emphasized. On the other hand, at sufficiently small angles, it is reasonable to expect that a very good approximation will be provided by the contribution of the Gaussian-like term of the scattering theory to the final expression for the energy-angle distribution of the photons. The treatment of this contribution which in I was called the "zeroth-order term" of the photon distribution was exact (in the frame work of the Schiff theory) in the case in which the screening of the nucleus by the outer electrons is neglected. On the other hand, the treatment of the screening and, more specifically, the determination of the "screening angles" χ_1 and χ_2 [Eqs. (9) and (9a) of I] were only approximative.

Both theoretical and experimental arguments may be advanced to show the necessity of a more detailed study of the betatron spectrum at small angles. In the case in which the characteristic width μ/E_0 of the bremsstrahlung distribution is small in comparison with the width of the multiple-scattering distribution [i.e., when $\lambda \ll 1$, see Eq. (2)], it is a well-known theoretical prediction that the shape of the spectrum is roughly independent of angle and is given approximately by the integrated spectrum of Schiff's intrinsic distribution.[4] This argument is valid for angles θ large in comparison with μ/E_0 (but not large in comparison with $\chi_c^2 B$), and it is based on the fact that, under those circumstances, the electron angular distribution is a very slowly varying function of angle so that it may be taken out of the convolution integrals. This, however, is not a very good approximation when $\theta \lesssim \mu/E_0$. As will be shown later,

* Supported in part by the joint program of the Office of Naval Research and the U. S. Atomic Energy Commission.

† A summary of some of the results of this paper were presented before the 1956 Washington meeting of the American Physical Society.

[1] A. Sirlin, Phys. Rev. **101**, 1219 (1956). Hereafter, this paper will be referred to as I.

[2] L. I. Schiff, Phys. Rev. **83**, 252 (1951).

[3] G. Molière, Z. Naturforsch. **3a**, 78 (1948); H. A. Bethe, Phys. Rev. **89**, 1256 (1953).

[4] L. I. Schiff, Phys. Rev. **70**, 87 (1946); J. D. Lawson, Nucleonics **10**, No. 11, 61 (1952). Of course, in that approximation the whole spectrum is multiplied by an angle-dependent function.

corrective terms arise because of the logarithmic peak of the scattering distribution at $\theta=0$, and these corrective terms modify the shape of the spectrum even for very small values of λ and, especially, for the low-energy quanta.[5] When θ increases well beyond μ/E_0, these corrective terms become negligible. For $\theta\lesssim\mu/E_0$ and $\lambda\ll1$, the corrections are largest in the region of complete screening and they are negligible in the region of no screening. The effect in the low-energy part of the spectrum is to give a value lower than that corresponding to the integrated spectrum of the intrinsic distribution.

All this points to the result that, for $\lambda\ll1$, the angular distribution (normalized to unity at $\theta=0$) of the spectral components corresponding to complete screening is somewhat broader than that of the components corresponding to no screening. (The magnitude of these predicted differences is not very large; see Fig. 3.)[6]

It is the aim of this paper to study the shape of the spectrum at small angles, taking a more detailed account of the influence of the screening on the basis of Schiff's distribution for the intrinsic bremsstrahlung. From the experimental standpoint, the interest of that study is based on the fact that in some of the modern accelerators, because of the large incident energies available, a considerable part of the spectrum lies on the region in which the screening is important. Moreover, there are already some indications of rather large variations in the experimental angular distribution of different components of betatron radiation.[7] This, again, indicates the necessity of a theory which may provide a more detailed description of the whole spectrum at small angles.

In order to maintain a reasonable mathematical simplicity, we shall limit ourselves to the treatment of the zeroth order term in the sense of I. We must bear in mind that this is justified only in the case of rather small angles ($\theta^2\lesssim\chi_c^2B$).

In Sec. B, a simple expression for the forward spectrum valid for any value of the screening parameter ρ [see Eq. (4a)] is developed in the case $\lambda\ll1$, keeping terms of order $\ln\lambda$ and terms independent of λ. Terms of order $\lambda(\ln\lambda)^2$ or higher are neglected. It will be apparent that the approximation of the forward spectrum by the integrated spectrum of the intrinsic distribution corresponds to keeping only terms of order $\ln(\gamma\lambda)$, where $\ln\gamma$ is Euler's constant.

In Sec. C, an expression for the angular distribution in the case of complete screening is exactly worked out, the results being expressed in terms of one-dimensional integrals which may be calculated numerically for any value of λ. In the case of the forward radiation, these integrals reduce to series which may be readily evaluated for $\lambda\lesssim1$ (Sec. D).

This, together with some of the results of I, provide simple and exact expressions (within the validity of the Schiff theory and the zeroth-order approximation) for the dependence of the forward spectrum on the target thickness T in the extreme cases of complete screening and no screening.

Finally, in Sec. E an expression for the forward spectrum is given for $\lambda\lesssim1$, which yields the same results as the exact treatment of Sec. D in the cases of complete screening and no screening and provides a good approximation in the case of intermediate screening.

A. GENERAL EXPRESSIONS

According to Eqs. (4), (2d), and (3) of I, the expression for the combined energy-angle distribution in the zeroth-order approximation reads

$$P(\vartheta)\vartheta d\vartheta=\vartheta d\vartheta NT\frac{d\eta}{\eta}\frac{2Z^2}{137}\left(\frac{e^2}{\mu}\right)^2\times\{(2-2\eta+\eta^2)K^{(0)}(\vartheta,\lambda)-(2-\eta)^2I^{(0)}(\vartheta,\lambda)+\tfrac{2}{3}(1-\eta)[4J^{(0)}(\vartheta,\lambda)-L^{(0)}(\vartheta,\lambda)]\},\quad(1)$$

where

$$I^{(0)}(\vartheta,\lambda)=F^{(0)}(\vartheta)*\frac{2}{\lambda}(1+\vartheta^2/\lambda)^{-2},\quad(1a)$$

$$J^{(0)}(\vartheta,\lambda)=F^{(0)}(\vartheta)*\frac{12\vartheta^2}{\lambda^2}(1+\vartheta^2/\lambda)^{-4},\quad(1b)$$

$$K^{(0)}(\vartheta,\lambda)=F^{(0)}(\vartheta)*\frac{2}{\lambda}(1+\vartheta^2/\lambda)^{-2}\ln M(\vartheta^2/\lambda),\quad(1c)$$

$$L^{(0)}(\vartheta,\lambda)=F^{(0)}(\vartheta)*\frac{12\vartheta^2}{\lambda^2}(1+\vartheta^2/\lambda)^{-4}\ln M(\vartheta^2/\lambda).\quad(1d)$$

Following the notation of I, the symbol $f(\vartheta)*g(\vartheta)$ means the convolution of $f(\vartheta)$ and $g(\vartheta)$ in the plane of ϑ, μ is the rest energy of the electron, η is the ratio of the photon energy k to the energy E_0 of the incident electron, T is the total target thickness, and

$$\vartheta=\theta/[\chi_c(T)B^{\frac{1}{2}}(T)]\quad(1e)$$

is Molière's reduced angle [θ is the geometrical angle and the functions $\chi_c(T)$ and $B(T)$ are given in the two papers of reference 3].

The parameter λ, defined by

$$\lambda=\mu^2/[E_0^2\chi_c^2(T)B(T)],\quad(2)$$

[5] The rather large deviation of the actual forward spectrum from the integrated spectrum was also found independently by numerical methods by E. Hisdal [Phys. Rev. **105**, 1821 (1957)].

[6] It is convenient to bear in mind that the region of complete screening extends from the low-energy limit of the photon spectrum up to values of the photon energy consistent with the condition $\rho\gg1$, ρ being the screening parameter defined in Eq. (4a). Similarly, the region of no screening extends from the high-energy limit up to a value of the photon energy consistent with the condition $\rho\ll1$.

[7] R. M. Warner and E. F. Shrader, Rev. Sci. Instr. **25**, 663 (1954).

measures the relative importance of the influence of multiple scattering on the final distribution of the photons: $\lambda\to 0$ means that the final angular distribution of the photons is essentially determined by the multiple scattering distribution while $\lambda\to\infty$ means that the influence of multiple scattering is negligible.[8] It should be noticed that for $E_0\gg\mu$, which is the case of interest here, $\chi_c^2 B$ varies with the energy as E_0^{-2}, so that λ is independent of E_0. In this case, then, λ is only a function of Z, the mass number A, and the total thickness T of the target.

In the zeroth-order approximation, according to Eqs. (2d) and (11) of I, the electron distribution reduces to

$$F^{(0)}(\vartheta)=2\int_0^1 \exp(-\vartheta^2/\tau)d\tau/\tau=-2\,\mathrm{Ei}(-\vartheta^2), \quad (3)$$

where $\mathrm{Ei}(-x)$ is the exponential integral as defined in Jahnke-Ende.[9] The distribution $F^{(0)}(\vartheta)\vartheta d\vartheta$ represents, of course, the total number of electrons which have been scattered through a reduced angle ϑ about the incident direction at any point of their path through the target.

The influence of the screening is contained in the function $M(\vartheta^2/\lambda)$, which is defined by the following expression:

$$\frac{1}{M(\xi)}=\left(\frac{Z^{\frac{1}{3}}}{111}\right)^2\left[\frac{1}{(1+\xi)^2}+\frac{1}{\rho^2}\right], \quad (4)$$

where

$$\rho=2\frac{E_0}{\mu}\frac{Z^{\frac{1}{3}}}{111}\left(\frac{1}{\eta}-1\right). \quad (4a)$$

The parameter ρ measures the relative importance of the screening in Schiff's theory: $\rho\ll 1$ means no screening while $\rho\gg 1$ means complete screening.

Equations (1), (1a), and (1b) correspond to Eqs. (5), (5a), and (5b) of I. Useful and exact expressions for $I^{(0)}(\vartheta,\lambda)$ and $J^{(0)}(\vartheta,\lambda)$ have been given in Eqs. (12), (13), (14), (14a), (B,5), and (B,9) of I. On the other hand, the evaluation of the functions $K^{(0)}(\vartheta,\lambda)$ and $L^{(0)}(\vartheta,\lambda)$ given in Eqs. (5), (9), and (9a) of I was only exact in the case of no screening. The influence of screening was taken into account only approximately.

In order to simplify the notation, the superscript (0) in the functions $I^{(0)}$, $J^{(0)}$, $K^{(0)}$, and $L^{(0)}$ will be omitted in the following sections. We must remember, however, that all the results of the present paper correspond to the zeroth-order approximation.

[8] The fact that the value of the function $\chi_c^2(t)B(t)$ is taken at $t=T$ has been mathematically justified in paper I [discussion after Eq. (8) of I]. If the use of any other Gaussian-like theory of multiple scattering is desired, it is sufficient to replace in Eq. (2) the quantity $\chi_c^2(T)B(T)$ by the square of the width of such distribution law.

[9] E. Jahnke and F. Emde, *Tables of Functions* (Dover Publications, New York, 1945).

B. FORWARD SPECTRUM FOR $\lambda\ll 1$

In the case of the forward radiation ($\vartheta=0$), the following exact expressions valid for all values of λ have been derived in I:

$$I(0,\lambda)/2=-e^{\lambda}\,\mathrm{Ei}(-\lambda), \quad (5)$$

$$J(0,\lambda)/2=-e^{\lambda}\,\mathrm{Ei}(-\lambda)(1-\lambda-\lambda^2)+\lambda. \quad (5a)$$

$$-\mathrm{Ei}(-\lambda)\equiv\int_\lambda^\infty \frac{e^{-t}}{t}dt.$$

In that case, it is easily seen that Eqs. (1c) and (1d) reduce to

$$K(0,\lambda)=-2\int_0^\infty \mathrm{Ei}(-\lambda\xi)(1+\xi)^{-2}\ln M(\xi)d\xi, \quad (6)$$

$$L(0,\lambda)=-12\int_0^\infty \mathrm{Ei}(-\lambda\xi)\xi(1+\xi)^{-4}\ln M(\xi)d\xi. \quad (6a)$$

In principle, these integrals may be worked out numerically. Unfortunately, they involve three parameters, Z, λ, and ρ, spreading over a very large range of values of experimental interest, so that such a tabulation would be very laborious.

In this section, expressions valid for $\lambda\ll 1$ will be given keeping terms of order $\ln\lambda$ and terms independent of λ. Terms of order λ, $\lambda(\ln\lambda)^2$, $\lambda\ln\lambda$, or higher will be neglected. In this case, $I(0,\lambda)$ and $J(0,\lambda)$ reduce to $-2\ln(\gamma\lambda)$, where $\ln\gamma$ is Euler's constant. The neglect of terms of order λ, $\lambda\ln\lambda$, and higher is equivalent to the replacement of $\mathrm{Ei}(-\lambda\xi)$ by $\ln(\gamma\lambda\xi)$ in Eqs. (6) and (6a), so that

$$K(0,\lambda)=-2\int_0^\infty \ln(\gamma\lambda\xi)(1+\xi)^{-2}\ln M(\xi)d\xi + O(\lambda,\lambda\ln\lambda\cdots), \quad (6b)$$

$$L(0,\lambda)=-12\int_0^\infty \ln(\gamma\lambda\xi)\xi(1+\xi)^{-4}\ln M(\xi)d\xi + O(\lambda,\lambda\ln\lambda\cdots). \quad (6c)$$

These integrals may be solved exactly by partial integrations or by contour methods, and the following results are obtained:

$$K(0,\lambda)=-2\ln(\gamma\lambda)[\ln M(0)+2-2\tan^{-1}\rho/\rho] + G_1(\rho)+O(\lambda,\lambda\ln\lambda\cdots), \quad (7)$$

$$L(0,\lambda)=-2\ln(\gamma\lambda) \times\left[\ln M(0)+\frac{4}{\rho^2}-\frac{3}{\rho^2}\ln(1+\rho^2)-\frac{4}{\rho^3}\tan^{-1}\rho+5/3\right] + G_2(\rho)+O(\lambda,\lambda\ln\lambda\cdots), \quad (7a)$$

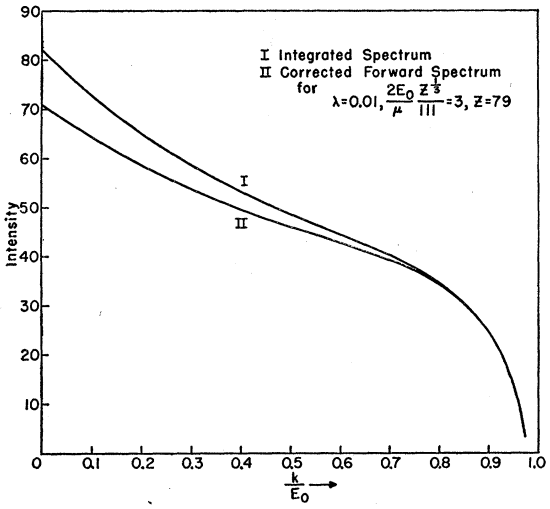

FIG. 1. Comparison between the integrated intensity spectrum of the intrinsic distribution [multiplied by $-2\ln(\gamma\lambda)$] with the forward intensity (as given in Sec. B) in the case $Z=79$, $\lambda=0.01$, and $2E_0Z^{\frac{1}{3}}/(111\mu)=3$. The latter is calculated on the basis of Eq. (1) (expression between curly brackets), and Eqs. (7) *et seq.*, in which terms of order λ and higher are neglected.

where

$$G_1(\rho)=\ln(1+\rho^2)\left[\tfrac{1}{2}\ln(1+\rho^2)+\frac{2}{\rho}\tan^{-1}\rho\right]-2(\tan^{-1}\rho)^2-F(\rho^2), \quad (7b)$$

$$G_2(\rho)=\ln(1+\rho^2)\left[\tfrac{1}{2}\ln(1+\rho^2)\left(\frac{3}{\rho^2}+1\right)+\frac{4}{\rho^3}\tan^{-1}\rho+\frac{2}{\rho^2}\right\}-2(\tan^{-1}\rho)^2\left(1+\frac{3}{\rho^2}\right)+4-\frac{4}{\rho}\tan^{-1}\rho-F(\rho^2). \quad (7c)$$

Here $F(y)$ is the Spence's function defined by

$$F(y)=\int_0^y \ln(1+t)dt/t. \quad (7d)$$

Useful expressions for the evaluation of $F(y)$ are given in Appendix A.[10]

If the contributions of $G_1(\rho)$, $G_2(\rho)$, and the terms of order $\lambda, \lambda\ln\lambda, \cdots$, are neglected in Eqs. (7) and (7a), the forward spectrum given by Eq. (1) is proportional to the integrated spectrum of the intrinsic distribution, which is the approximation used in the literature.[4] Thus, for $\lambda\ll1$, the functions $G_1(\rho)$ and $G_2(\rho)$ give the main deviation from the integrated spectrum.

In the case of no screening ($\rho\to0$), $G_i(\rho)\to0$ ($i=1,2$).[11] For complete screening ($\rho\to\infty$), $G_1(\infty)=-\frac{2}{3}\pi^2$ and $G_2(\infty)=4-\frac{2}{3}\pi^2$. For finite ρ, the values of $G_i(\rho)$ lie between zero and these two extremes.

In Fig. 1, the effect of the corrections $G_i(\rho)$ is illustrated for a particular case. The intensity spectrum given by Eq. (1) (expression between curly brackets) and Eqs. (7) *et seq.* is compared with the integrated intensity spectrum of the intrinsic distribution multiplied by $-2\ln(\gamma\lambda)$. The latter is given by the expression between curly brackets in Eq. (3) of reference 2. It is apparent that the deviations from the integrated spectrum are appreciable for low- and intermediate-energy quanta.

The main limitation of the results of this section is the fact that the terms of order $\lambda, \lambda\ln\lambda, \cdots$ have been neglected. Fortunately, these higher order terms in the expression for the forward radiation may be worked out exactly in the extreme cases of no screening and complete screening. The results for these two limiting cases will be shown in Sec. D.

C. COMPLETE SCREENING, ANGULAR DISTRIBUTION

In this section, the problem of the angular distribution is studied in the extreme case of complete screening ($\rho\gg1$). The importance of this limiting case is based, of course, on the fact that in some of the modern accelerators, because of the high energies available for the incident electrons, a considerable part of the photon spectrum lies in the region $\rho\gg1$.

In the limit $\rho\to\infty$, when one remembers Eqs. (1a) and (4), it is clear that Eq. (1c) reduces to

$$K(\vartheta,\lambda)=2\ln(111/Z^{\frac{1}{3}})I(\vartheta,\lambda)+F(\vartheta)*(4/\lambda)(1+\vartheta^2/\lambda)^{-2}\ln(1+\vartheta^2/\lambda). \quad (8)$$

In order to evaluate the integral of Eq. (8), use is made of the folding theorem for the Bessel function J_0. Remembering Eq. (3) and using the well-known expression for the Bessel (Fourier) transform of the Gaussian function [see Eq. (B1) of Appendix B], we get

$$g(y)=\int_0^\infty J_0(y\vartheta)F(\vartheta)\vartheta d\vartheta=\int_0^1 \exp(-y^2\tau/4)d\tau. \quad (8a)$$

The Bessel transform of the second folding factor of Eq. (8) admits the following integral representation (see Appendix B):

$$h(y)=\frac{4}{\lambda}\int_0^\infty J_0(y\vartheta)(1+\vartheta^2/\lambda)^{-2}\ln(1+\vartheta^2/\lambda)\vartheta d\vartheta$$
$$=-2\int_0^\infty \exp\left(-\alpha-\frac{y^2\lambda}{4\alpha}\right)\ln\alpha d\alpha+2\psi(1)\int_0^\infty \exp\left(-\alpha-\frac{y^2\lambda}{4\alpha}\right)d\alpha, \quad (8b)$$

[10] Tables of $F(y)$ as well as useful relations involving this function are given by K. Mitchell, Phil. Mag. **40**, 351 (1949).

[11] The fact that $G_i(\rho)$ ($i=1, 2$) vanish for $\rho=0$ may be easily understood mathematically as follows. It is clear that the $G_i(\rho)$ come from the contribution of $\ln\xi$ in Eqs. (6b) and (6c). Now, for $\rho\to0$, $\ln M(\xi)$ is independent of ξ, so that $\ln\xi$ contributes integrals of the form $\int_0^\infty(1+\xi^2)^{-2n}\xi^{2n-1}\ln\xi d\xi$, where n is a positive integer. It is easy to see that these integrals vanish.

where $\psi(1)$ is the logarithmic derivative of the factorial function as defined in Jahnke-Ende. By virtue of the folding theorem, we get

$$F(\vartheta)*(4/\lambda)(1+\vartheta^2/\lambda)^{-2}\ln(1+\vartheta^2/\lambda)$$
$$=\int_0^\infty J_0(\vartheta y)h(y)g(y)ydy. \quad (8c)$$

Observing Eqs. (8a) and (8b), we notice that in Eq. (8c) the integration over y is essentially the Bessel transform of a Gaussian function, so that it may be carried out immediately using Eq. (B1). By remembering the integral representation of $I(\vartheta,\lambda)$ given in Eq. (10) of I and performing the integration over τ, the following result is finally obtained:

$$K(\vartheta,\lambda)=2\left[\ln\left(\frac{111}{Z^{\frac{1}{3}}}\right)+\psi(1)\right]I(\vartheta,\lambda)$$
$$-4\int_0^\infty e^{-\alpha}\ln\alpha\left[\mathrm{Ei}\left(-\frac{x\alpha}{\lambda}\right)-\mathrm{Ei}\left(-\frac{x\alpha}{\alpha+\lambda}\right)\right]d\alpha, \quad (9)$$

where $x=\vartheta^2$. An analogous method leads to

$$L(\vartheta,\lambda)=2\left[\ln\left(\frac{111}{Z^{\frac{1}{3}}}\right)+\psi(3)\right]J(\vartheta,\lambda)$$
$$-4\int_0^\infty e^{-\alpha}\alpha\ln\alpha\left[\mathrm{Ei}\left(-\frac{x\alpha}{\lambda}\right)-\mathrm{Ei}\left(-\frac{x\alpha}{\alpha+\lambda}\right)\right.$$
$$\left.+\frac{\lambda}{\alpha+\lambda}\exp\left(-\frac{x\alpha}{\alpha+\lambda}\right)-\exp\left(-\frac{x\alpha}{\lambda}\right)\right]d\alpha. \quad (9a)$$

The integrals involving $\mathrm{Ei}(-x\alpha/\lambda)$ and $\exp(-x\alpha/\lambda)$ in Eqs. (9) and (9a) may be easily reduced to closed form (see Appendix C). However, no simple closed expressions for the integrals involving $\mathrm{Ei}(-x\alpha/(\alpha+\lambda))$ have been found. For a given value of x and λ, the expressions in Eqs. (9) and (9a) may be evaluated simply by a combination of numerical and analytical methods (see Appendix C).

In Fig. 2, the intensity spectra predicted by Eq. (1) (expression between curly brackets) and Eqs. (9) and (9a) for $\lambda=0.01$ at various angles are compared with the approximation in which the energy-angle distribution is represented by the integrated spectrum multliplied by the angle dependent function $-2\,\mathrm{Ei}(-x-\lambda)$. Strictly speaking, the approximation used in the literature, in which the electron distribution $F(\vartheta)$ is regarded as slowly varying in comparison with the intrinsic photon distribution $\sigma(\vartheta)$ leads to an energy-angle distribution given by the integrated spectrum multiplied by $F(\vartheta)$. However, as $F(\vartheta)$ diverges at $\vartheta=0$, in order to compare that approximation with the exact results of this section, the next best choice has been of replacing

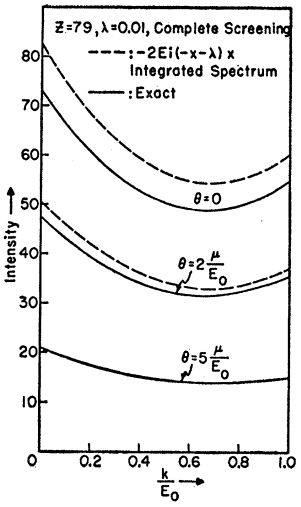

FIG. 2. Comparison of the integrated spectrum approximation with the exact results at various angles in the case $\lambda=0.01$, $Z=79$ and complete screening. The latter are calculated on the basis of Eqs. (12) and (13) of I and Eqs. (1), (9), (9a), and (C,4) of this paper.

$F(\vartheta)$ by $-2\,\mathrm{Ei}(-x-\lambda)$, that gives the value quoted in the literature for $\vartheta=0$ and $\lambda\ll1$ and is a good approximation of the functions $I(\vartheta)$ and $J(\vartheta)$ for $\lambda\ll1$ and $\vartheta\lesssim1$ [see Eqs. (12) and (13) of I]. We see that the difference between this approximation and the exact results is largest for $\theta=0$, is rather small for $\theta=2\mu/E_0$, and is negligible for $\theta=5\mu/E_0$.

This behavior is easily understood as follows. The integrated spectrum approximation is based on the fact that, for $\lambda\ll1$, the electron distribution $F(\vartheta)$ is a very slowly varying function of angle in comparison with the intrinsic distribution (which in the limit $\lambda\to0$ behaves like a δ distribution), so that it may be taken out of the convolution integrals. This argument is valid for angles θ larger than μ/E_0 [but not large in comparison with $\chi_c(T)B^{\frac{1}{2}}(T)$; see below]. When $\theta\lesssim\mu/E_0$, this is not a good approximation because of the logarithmic divergence of $F(\vartheta)$ at $\vartheta=0$.

In order to have a more physical picture, let us first limit ourselves to the case $\theta=0$. Most of the radiation at $\theta=0$ comes from a cone of width μ/E_0 about that direction. Now, as shown by the logarithmic peak of $F(\vartheta)$ at $\vartheta=0$, in that cone the electrons are predominantly scattered in the forward direction. This means that the contribution to the total forward radiation of the forward-emitted photons is more heavily weighted than that of the photons emitted through a finite angle. This explains the deviation of the forward spectrum from the integrated spectrum. As we see from Figs. 1 and 2, the exact calculations in the region of complete screening give at $\vartheta=0$ a value lower than that corresponding to the integrated spectrum. If we now consider the final radiation at an angle θ well beyond μ/E_0, the forward-scattered electrons will not contribute. Then, if $\lambda\ll1$, $F(\vartheta)$ will be nearly a constant in the interval of width μ/E_0 about θ, so that the contribution of all the photons will be equally weighted throughout that cone. Thus, in this case, we may expect the exact solution to coincide with the integrated spectrum ap-

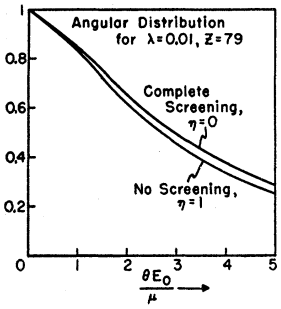

FIG. 3. Comparison of the angular distribution (normalized to 1 at $\theta=0$) for complete screening and no screening in the case $Z=79$ and $\lambda=0.01$. The curve for complete screening is calculated for $\eta=0$ and may be read partially from Fig. 2. The curve for no screening is calculated for $\eta=1$, in which case it is given exactly by $I(\vartheta)/I(0)$ [Eq. (12) of I].

proximation, as is shown in Fig. 2 for the case of complete screening.

For $\theta>\chi_c B^{\frac{1}{2}}$, this intuitive discussion is complicated by the fact that the zeroth-order approximation [Eq. (3)] is not correct and the terms of order B^{-1} must be taken into account [see Eq. (2d) of I]. In that case the final distribution is influenced by the relative values of the parameters λ and B^{-1}. We shall not enter however, into a discussion of this region.

On the other hand, in the case of no screening and $\lambda\ll 1$, the integrated spectrum approximation is very good even for the forward radiation. This is connected with the rather fortuitous cancellation of the functions $G_i(\rho)$ for $\rho\to 0$ (see footnote 11).

As a consequence of the discussion given above, we should expect the angular distribution (normalized to unity at zero angle) to be somewhat broader for the spectral components corresponding to complete screening than for the components corresponding to no screening (see reference 6). This is illustrated in Fig. 3 for $\lambda=0.01$. The curve for complete screening has been calculated for the spectral component $\eta=0$ from Eqs. (1), (9), and (9a) and may be also partially obtained from Fig. 2. The curve for no screening has been calculated for $\eta=1$ and is then given by the function $I(\vartheta,\lambda)$ [Eq. (12) of I]. It is seen that, for $\lambda=0.01$, the difference between these two extreme cases is not very large, being at most of the order of ten percent. For the case of intermediate screening, the angular distribution for $\lambda=0.01$ is expected to lie between the two curves of Fig. 3.

D. COMPLETE SCREENING, FORWARD SPECTRUM

In the cases of the forward radiation ($\vartheta=0$), Eqs. (9) and (9a) reduce to

$$K(0,\lambda)/4=[\ln(111/Z^{\frac{1}{3}})+\psi(1)]\times I(0,\lambda)/2-X(\lambda),\quad \text{C.S.} \tag{10}$$

$$L(0,\lambda)/4=[\ln(111/Z^{\frac{1}{3}})+\psi(3)]J(0,\lambda)/2+\lambda[X(\lambda)+I(0,\lambda)/2]+\psi(1)-(1+\lambda)Y(\lambda),\quad \text{C.S.} \tag{10a}$$

where the abbreviations C.S. mean complete screening and

$$X(\lambda)=\int_0^\infty e^{-\alpha}\ln\alpha\ln(1+\alpha/\lambda)d\alpha, \tag{10b}$$

$$Y(\lambda)=\int_0^\infty e^{-\alpha}\alpha\ln\alpha\ln(1+\alpha/\lambda)d\alpha. \tag{10c}$$

For $\lambda\lesssim 1$, these integrals may be readily computed from the following exact expressions, whose derivation is sketched in Appendix D:

$$X(\lambda)=\mathrm{Ei}(-\lambda)[\bar{\mathrm{E}}\mathrm{i}(\lambda)-\ln(\gamma\lambda)]+e^\lambda[\mathrm{Ei}(-\lambda)-\ln\lambda][\mathrm{Ei}(-\lambda)-\ln(\gamma\lambda)]+\tfrac{1}{2}(e^\lambda+1)[\tfrac{1}{6}\pi^2+(\ln\gamma)^2]+\tfrac{1}{2}(1-e^\lambda)(\ln\lambda)^2+\ln\gamma\ln\lambda+e^\lambda\sum_{n=1}^{\infty}\frac{(-\lambda)^n}{n!n^2}+\sum_{n=1}^{\infty}(-\lambda)^n S_n \tag{10d}$$

$$Y(\lambda)=\mathrm{Ei}(-\lambda)[\bar{\mathrm{E}}\mathrm{i}(\lambda)-\ln(\gamma\lambda)]+e^\lambda[\mathrm{Ei}(-\lambda)-\ln\lambda][\mathrm{Ei}(-\lambda)-\ln(\gamma\lambda)][1-\lambda]+\tfrac{1}{2}[e^\lambda(1-\lambda)+1][\tfrac{1}{6}\pi^2+(\ln\gamma)^2]-(1+e^\lambda)\ln(\gamma\lambda)-\tfrac{1}{2}[e^\lambda(1-\lambda)-1](\ln\lambda)^2+(1+\ln\gamma)\ln\lambda-e^\lambda\sum_{n=2}^{\infty}\frac{(-\lambda)^n}{(n-2)!}\left[\frac{1}{n^3}-\frac{1}{(n-1)^3}\right]-\sum_{n=2}^{\infty}(-\lambda)^n P_n, \tag{10e}$$

where

$$S_n=\sum_{\nu=n+1}^{\infty}\frac{(\nu-n-1)!}{\nu!}\sum_{\mu=1}^{\nu-1}\frac{1}{\mu}, \tag{10f}$$

$$P_n=(n-1)S_n-\frac{1}{n!}\sum_{\mu=1}^{n-1}\frac{1}{\mu}, \tag{10g}$$

and $\bar{\mathrm{E}}\mathrm{i}(\lambda)$ is defined in Jahnke and Emde.[9]

In Appendix D, a simple and exact method to evaluate the leading S_n is explained. The results up to $n=4$ are the following:

$$S_1=\tfrac{1}{6}\pi^2;\quad S_2=\tfrac{1}{4}(5-\tfrac{1}{3}\pi^2);\quad S_3=\tfrac{1}{6}(\tfrac{1}{6}\pi^2-1);\quad S_4=\frac{1}{4!6}\left(\frac{157}{12}-\pi^2\right). \tag{10h}$$

TABLE I. The functions $X(\lambda)$, $Y(\lambda)$, $1+\xi_1(\lambda)$, and $1+\xi_2(\lambda)$.

λ	$X(\lambda)$	$Y(\lambda)$	$1+\xi_1(\lambda)$	$1+\xi_2(\lambda)$
0.01	−0.849	2.766	1.880	1.971
0.019	−0.568		1.797	
0.03	−0.389	2.293	1.734	1.884
0.055	−0.187		1.644	
0.1	−0.0339	1.764	1.552	1.749
0.17	0.0615		1.469	
0.3	0.122	1.274	1.382	1.587
0.6	0.144		1.282	
1.0	0.134	0.764	1.213	1.387

The functions $X(\lambda)$ and $Y(\lambda)$ are plotted in Fig. 4 as functions of $\ln\lambda$ in the range $0.01\leq\lambda\leq 1$ (see also Table I). In that region $Y(\lambda)$ may be represented very accurately by a linear function of $\ln\lambda$.

Equations (1), (5), and (5a) together with Eqs. (1) *et seq.* provide an exact expression (in the framework of the Schiff's theory and the zeroth-order approximation) for the forward spectrum in the case of complete screening. The corresponding results for the case of no screening are given by Eqs. (1), (5), and (5a), and by the relations:

$$K(0,\lambda)=\ln M(Z=0)I(0,\lambda), \quad \text{N.S.} \quad (11)$$

$$L(0,\lambda)=\ln M(Z=0)J(0,\lambda). \quad \text{N.S.} \quad (11a)$$

E. INTERMEDIATE SCREENING, FORWARD RADIATION

In this section, an expression is given for the forward spectrum, which yields the same results as the exact treatment of Sec. D in the cases of complete and no screening and provides a good approximation in the region of intermediate screening.

According to Eqs. (4) and (6), we may write

$$K(0,\lambda)=K(0,\lambda)_{\text{C.S.}}$$
$$+2\int_0^\infty \mathrm{Ei}(-\lambda\xi)(1+\xi)^{-2}\ln[1+(1+\xi)^2/\rho^2]d\xi$$
$$=K(0,\lambda)_{\text{C.S.}}-\ln[1+(1+\xi_1)^2/\rho^2]I(0,\lambda), \quad (12)$$

where ξ_1 is a certain intermediate value of ξ and $K(0,\lambda)_{\text{C.S.}}$ is the expression for $K(0,\lambda)$ in the case of complete screening [see Eq. (10)]. Equation (12) gives automatically the correct answer for the case of complete screening ($\rho\to\infty$). The idea of the approximation is, then, to determine the intermediate value by requiring the right hand member of Eq. (12) to coincide also with the correct result in the limiting case of no screening ($\rho\ll 1$). In the latter case, it is easily seen from Eqs. (4) and (11) that

$$K(0,\lambda)_{\text{N.S.}}=2\ln(111\rho/Z^{\frac{1}{3}})I(0,\lambda). \quad (12a)$$

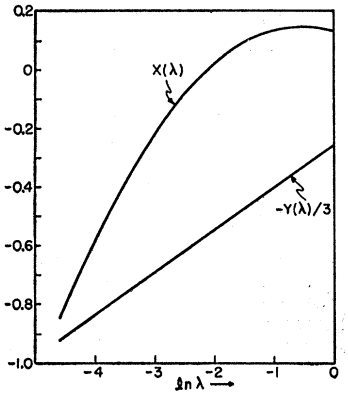

FIG. 4. The functions $X(\lambda)$ and $Y(\lambda)$.

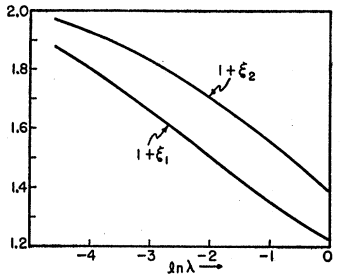

FIG. 5. The functions $1+\xi_1(\lambda)$ and $1+\xi_2(\lambda)$.

Now we require the right-hand member of Eq. (12) to coincide with Eq. (12a) in the limit $\rho\to 0$. Remembering Eq. (10), we find that ξ_1 is determined by the following relation:

$$\ln(1+\xi_1)=\psi(1)-2X(\lambda)/I(0,\lambda). \quad (12b)$$

The solution of this equation is plotted in Fig. 5 as a function of $\ln\lambda$ and we notice that it behaves practically as a straight line in the region $0.01\leq\lambda\leq 1$. In fact, with an accuracy of a few percent, we may approximate $1+\xi_1(\lambda)$ in that region by the formula[12]

$$1+\xi_1(\lambda)\cong 1.22-0.143\ln\lambda \quad \text{for} \quad 0.01\leq\lambda\leq 1. \quad (12c)$$

A short table of $1+\xi_1$ as a function of λ is given in Table I. One way of testing the validity of this approximation in the region of intermediate screening, is to compare the predictions of Eqs. (12) and (12b) with those of Eq. (7) for $\lambda\ll 1$. This comparison has been made for $\lambda=0.01$ and the difference has been found to be less than one percent throughout the whole spectrum.[13] Equations (12) and (12b) have been also compared with the value of $K(0,\lambda)$ calculated by numerical integration for $\rho=1$ and $\lambda=1$ and the error was found to be a fraction of a percent.

An analogous approximation for $L(0,\lambda)$ is given by

$$L(0,\lambda)=L(0,\lambda)_{\text{C.S.}}-\ln[1+(1+\xi_2)^2/\rho^2]J(0,\lambda). \quad (13)$$

The function $1+\xi_2$ is plotted in Fig. 5 as a function of $\ln\lambda$ (see also Table I).

The forward intensity spectra given by Eq. (1) (expression between curly brackets) and Eqs. (5), (5a), (12), and (13) for three different value of λ is illustrated in Fig. 6 in the case $Z=79$ and $2E_0Z^{\frac{1}{3}}/(111\mu)=3$. The curve for $\lambda=0.1$ is also compared with the forward and integrated intensity spectra calculated from Schiff's intrinsic distribution. These are given by the expressions between curly brackets in Eqs. (1) and (3) of reference 2, respectively. In Fig. 6, the integrated spec-

[12] If one so desires, one may use Eq. (12c) to obtain an approximate closed expression for the function $X(\lambda)$. Inserting Eq. (12c) back into Eq. (12b), the following approximation for $X(\lambda)$ is obtained in the range $0.01\leq\lambda\leq 1$: $X(\lambda)\cong[\ln(1.22-0.143\ln\lambda)-\psi(1)]e^\lambda\,\mathrm{Ei}(-\lambda)$.

[13] In making this comparison, we have replaced in Eq. (12) the exact $K(0,\lambda)_{\text{C.S.}}$ by the approximate value given by Eq. (7) for $\rho\to\infty$. The difference between these two values is due, of course, to the neglect in Sec. B of terms of order $\lambda,\lambda\ln\lambda,\cdots$.

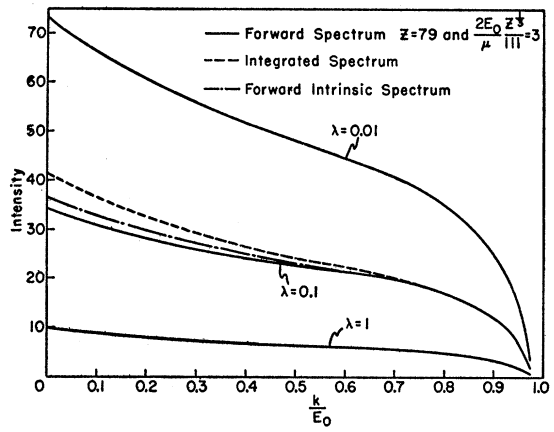

FIG. 6. Forward intensity spectra for various values of λ in the case $Z=79$ and $2E_0Z^{\frac{1}{3}}/(111\mu)=3$. The curves are calculated on the basis of Eqs. (1), (5), (5a), (12), and (13).

trum has been normalized to the value of the corrected spectrum at the maximum value of η, i.e., at $\eta_{\max}=1-\mu/E_0$. Then the forward intrinsic spectrum is normalized so as to preserve the original ratio to the integrated spectrum (in our case the difference between the two last distributions is still significant at $\eta_{\max}\cong 0.975$, although they are identical for an hypothetical value of $\eta_{\max}=1$). It is seen that the integrated spectrum lies above the forward intrinsic spectrum, the difference being greatest at $\eta=0$ (about 12%). On the other hand, the corrected spectrum lies below the forward intrinsic spectrum in the low and intermediate energy region. This shows that in this region the forward intrinsic spectrum is a better approximation than the integrated spectrum. In the high-energy region, however, the corrected spectrum is better approximated by the integrated spectrum, though this cannot be observed in Fig. 6. An analogous comparison with the two corrected spectra for $\lambda=1$ and $\lambda=0.01$ leads to identical conclusions.

This behavior of the normalized curves of Fig. 6 may be understood again on the basis of the intuitive argument used in Sec. C to explain the behavior of the curves of Figs. 2 and 3. If by $\sigma(\theta,\eta)$ we represent the intrinsic distribution, then it is easily seen that, in our case and for small values of η, $\sigma(\theta,\eta)\sigma(0,\eta_{\max})/[\sigma(\theta,\eta_{\max})\sigma(0,\eta)]$ first decreases when θ varies from zero up to a certain small angle and then it begins to increase with θ to such an extent that the sum over angles of $\sigma(\theta,\eta)$ (integrated spectrum) lies appreciably above the value for $\theta=0$, if the normalization described above is used. On the other hand, when we take into account the influence of multiple scattering, the contribution to the forward radiation of photons emitted at small angles is weighted more heavily than that of those emitted at larger angles. This may yield, then, a value lower than that of the intrinsic forward spectrum. For $\lambda\to\infty$ ($T\to 0$), of course, the weighting factor behaves like a δ distribution, so that in that limit the actual spectrum coincides with the forward intrinsic spectrum, as expected.

ACKNOWLEDGMENTS

The author wishes to express his indebtedness to Professor G. Molière for his suggestions and observations, and to Professor A. Nordsieck for some discussions on this problem.

APPENDIX A

The following are useful expressions for the evaluation of the function $F(y)$ defined in Eq. (7d)

$$F(y)=-\sum_{n=1}^{\infty}\frac{(-y)^n}{n^2} \quad \text{for} \quad |y|\leq 1, \quad \text{(A1)}$$

$$F(y)=\tfrac{1}{6}\pi^2+\tfrac{1}{2}(\ln y)^2-F(1/y) \quad \text{for} \quad y\geq 1, \quad \text{(A2)}$$

$$F(y)=-F\left(-\frac{y}{1+y}\right)+\tfrac{1}{2}[\ln(1+y)]^2 \quad \text{for} \quad y\geq 0. \quad \text{(A3)}$$

Use of the relation (A3) is convenient when $0.5<y<1$.

APPENDIX B

Consider the Bessel (Fourier) transform of the Gaussian function

$$\frac{4}{\lambda}\int_0^{\infty}\vartheta d\vartheta J_0(y\vartheta)\exp\left(-\frac{\vartheta^2\alpha}{\lambda}\right)=\frac{2}{\alpha}\exp\left[-\frac{y^2\lambda}{(4\alpha)}\right]. \quad \text{(B1)}$$

By multiplying Eq. (B1) by $\alpha^{p-1}\exp(-\alpha)$ and integrating with respect to α from 0 to ∞, we get

$$\frac{4}{\lambda}\int_0^{\infty}\vartheta d\vartheta J_0(y\vartheta)\left(1+\frac{\vartheta^2}{\lambda}\right)^{-p}=\frac{2}{(p-1)!}\int_0^{\infty}\exp\left[-\alpha-\frac{y^2\lambda}{(4\alpha)}\right]\alpha^{p-2}d\alpha. \quad \text{(B2)}$$

By differentiating both members of Eq. (B2) with respect to p and then setting $p=2$, Eq. (8b) is obtained.

APPENDIX C

The method which we found most convenient for evaluating the integral of Eq. (9) is the following. The range of integration is divided into two intervals, one from $\alpha=0$ up to a value $\alpha_1\gg\lambda$ (say up to $\alpha_1=10\lambda$), and then from α_1 up to ∞. The integration over the first region is carried out numerically using the difference between the two exponential integrals and considering sufficiently small intervals. The integration over the second interval involving $\mathrm{Ei}[-x\alpha/(\alpha+\lambda)]$ may be

calculated by means of the expansion

$$\mathrm{Ei}[-x\alpha/(\alpha+\lambda)]=\mathrm{Ei}(-x)-e^{-x}\lambda/\alpha+\tfrac{1}{2}(\lambda/\alpha)^2e^{-x}[1-x]-\tfrac{1}{6}(\lambda/\alpha)^3e^{-x}[x^2-4x+2]+\cdots. \quad \text{(C1)}$$

If $\alpha_1=10\lambda$, the integrals originated by this expansion are elementary and converge very rapidly. The integration over the interval $\alpha_1\leq\alpha\leq\infty$ involving $\mathrm{Ei}(-x\alpha/\lambda)$ may be calculated by using the well-known series expansion for $\mathrm{Ei}(-x)$ (see reference 9, page 1 *et seq.*). For the sake of completeness, we give now the exact results for the integrals involving $\mathrm{Ei}(-x\alpha/\lambda)$ from 0 to ∞, which can be given in closed form:

$$\Lambda_1=\int_0^\infty e^{-\alpha}\ln\alpha\,\mathrm{Ei}\left(-\frac{x\alpha}{\lambda}\right)d\alpha=F\left(-\frac{x}{x+\lambda}\right)+\ln\left(1+\frac{\lambda}{x}\right)\ln\gamma+\frac{\pi^2}{6}, \quad \text{(C2)}$$

$$\Lambda_2=\int_0^\infty e^{-\alpha}\alpha\ln\alpha\,\mathrm{Ei}\left(-\frac{x\alpha}{\lambda}\right)d\alpha=\Lambda_1-\ln\left[\gamma\left(1+\frac{\lambda}{x}\right)\right]+\frac{1}{1+x/y}\left[(\ln\gamma)\frac{x}{\lambda}-\ln\left(1+\frac{x}{\lambda}\right)\right]. \quad \text{(C3)}$$

The energy-angle distribution depends much more sensitively on the function $K(\vartheta,\lambda)$ than on $L(\vartheta,\lambda)$. If $\lambda\ll1$, it is sometimes sufficient, then, to set $\lambda=0$ in the integration involving $\mathrm{Ei}[-x\alpha/(\alpha+\lambda)]$ in the evaluation of $L(\vartheta,\lambda)$, in which case we obtain the following approximate expression:

$$L(\vartheta,\lambda)\cong-[\ln(111/Z^{\frac{1}{3}})+\tfrac{5}{6}]\,\mathrm{Ei}(-\lambda-x)-\tfrac{1}{6}\pi^2-F\left(-\frac{x}{x+\lambda}\right)+\left[1+\frac{x}{\lambda}\right]^{-2}\times\left\{1+\frac{x}{\lambda}\ln\left[\gamma\left(1+\frac{x}{\lambda}\right)\right]\right\}. \quad \text{(C4)}$$

Because of the approximations involved, Eq. (C4) has not the proper asymptotic behavior for large x (it should behave asymptotically as x^{-3}), so that Eq. (C4) is not valid for $x\gg\lambda$. A similar simplification in the evaluation of $K(\vartheta,\lambda)$ would lead to a much poorer approximation. This is due to the fact that setting $\lambda=0$ in the integration involving $\mathrm{Ei}[-x\alpha/(\alpha+\lambda)]$ introduces a large error near $\alpha=0$. In the case of $L(\vartheta,\lambda)$, however, the additional factor α tends to diminish the contribution of that region. As the final energy-angle distribution depends very sensitively on $K(\vartheta,\lambda)$, it is convenient, then, to evaluate this function by using the accurate method described at the beginning of this appendix.

APPENDIX D

In order to evaluate $X(\lambda)$ [Eq. (10b)], we write

$$2X(\lambda)=\int_0^\infty e^{-\alpha}[\ln(\alpha+\lambda)]^2d\alpha+\int_0^\infty e^{-\alpha}(\ln\alpha)^2d\alpha-\int_0^\infty e^{-\alpha}\left[\ln\left(1+\frac{\lambda}{\alpha}\right)\right]^2d\alpha. \quad \text{(D1)}$$

The second integral is trivial. For evaluating the first integral, we introduce $u=\alpha+\lambda$ so that

$$\int_0^\infty e^{-\alpha}[\ln(\alpha+\lambda)]^2d\alpha=e^\lambda\int_\lambda^\infty e^{-u}(\ln u)^2du=e^\lambda\frac{\partial^2}{\partial p^2}\left[p!-\int_0^\lambda e^{-u}u^p du\right]_{p=0}. \quad \text{(D2)}$$

The integral in Eq. (D2) is simply expressed as a series in λ by expanding the exponential. The last integral in Eq. (D1) is evaluated by introducing $u=\alpha+\lambda$ and making use of the expansion

$$[\ln(1-u)]^2=2\sum_{n=2}^\infty\frac{u^n}{n}\sum_{\mu=1}^{n-1}\frac{1}{\mu} \quad \text{for} \quad |u|<1. \quad \text{(D3)}$$

Then, we get

$$\int_0^\infty e^{-\alpha}\left[\ln\left(1+\frac{\lambda}{\alpha}\right)\right]^2d\alpha=2e^\lambda\sum_{n=2}^\infty\frac{\lambda^n}{n}\sum_{\mu=1}^{n-1}\frac{1}{\mu}\int_\lambda^\infty\frac{e^{-u}}{u^n}du. \quad \text{(D4)}$$

The last expression is easily evaluated by partial integrations. An analogous method is used in the calculation of $Y(\lambda)$.

In order to evaluate exactly the leading S_n defined in Eq. (10f), the essential idea is to interchange the order of the summations. For example,

$$S_1=\sum_{\nu=2}^\infty\frac{1}{\nu(\nu-1)}\sum_{\mu=1}^{\nu-1}\frac{1}{\mu}=\sum_{\mu=1}^\infty\frac{1}{\mu}\sum_{\nu=\mu+1}^\infty\frac{1}{\nu(\nu-1)}. \quad \text{(D5)}$$

Observing that

$$\sum_{\nu=2}^\mu\frac{1}{\nu(\nu-1)}=\sum_{\nu=2}^\mu\left(\frac{1}{\nu-1}-\frac{1}{\nu}\right)=1-\frac{1}{\mu}, \quad \text{(D6)}$$

we see that Eq. (D5) reduces to

$$S_1=\sum_{\mu=1}^\infty\frac{1}{\mu^2}=\tfrac{1}{6}\pi^2.$$

A similar method has been used in the evaluation of S_2, S_3, and S_4.